

Metal–Organic Architectures Assembled from Multifunctional Polycarboxylates: Hydrothermal Self-Assembly, Structures, and Catalytic Activity in Alkane Oxidation

Jinzhong Gu,^{*,†} Min Wen,[†] Yan Cai,[†] Zifa Shi,[†] Aliaksandr S. Arol,[‡] Marina V. Kirillova,[‡] and Alexander M. Kirillov^{*,‡,§}

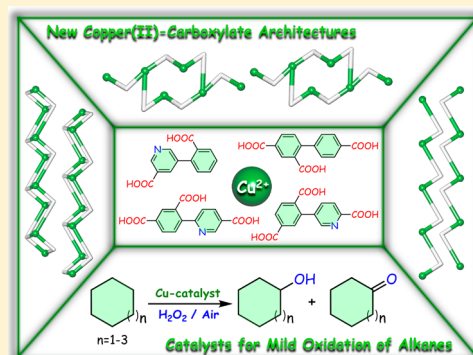
[†]State Key Laboratory of Applied Organic Chemistry, Key Laboratory of Nonferrous Metal Chemistry and Resources Utilization of Gansu Province, College of Chemistry and Chemical Engineering, Lanzhou University, Lanzhou 730000, People's Republic of China

[‡]Centro de Química Estrutural, Instituto Superior Técnico, Universidade de Lisboa, Avenida Rovisco Pais, 1049-001 Lisbon, Portugal

[§]Research Institute of Chemistry, Peoples' Friendship University of Russia (RUDN University), 6 Miklukho-Maklaya Street, Moscow 117198, Russian Federation

Supporting Information

ABSTRACT: A three-component aqueous reaction system comprising copper(II) acetate (metal node), poly(carboxylic acid) with a phenylpyridine or biphenyl core (main building block), and 1,10-phenanthroline (crystallization mediator) was investigated under hydrothermal conditions. As a result, four new coordination compounds were self-assembled, namely, $\{[\text{Cu}(\mu_3\text{-cpna})(\text{phen})]\cdot\text{H}_2\text{O}\}_n$ (1), $\{[\text{Cu}(\mu\text{-Hbtc})(\text{phen})]\cdot\text{H}_2\text{O}\}_n$ (2), $\{[\text{Cu}(\mu_3\text{-Hcpic})(\text{phen})]\cdot 2\text{H}_2\text{O}\}_n$ (3), and $[\text{Cu}_6(\mu\text{-Hcptc})_6(\text{phen})_6]\cdot 6\text{H}_2\text{O}$ (4), where H_2cpna = 5-(2'-carboxylphenyl)nicotinic acid, H_3btc = biphenyl-2,4,4'-tricarboxylic acid, H_3cpic = 4-(5-carboxypyridin-2-yl)isophthalic acid, H_3cptc = 2-(4-carboxypyridin-3-yl)terephthalic acid, and phen = 1,10-phenanthroline. Crystal structures of compounds 1–3 reveal that they are 1D coordination polymers with a ladder, linear, or double-chain structure, while product 4 is a 0D hexanuclear complex. All of the structures are extended further [1D \rightarrow 2D (1 and 2), 1D \rightarrow 3D (3), and 0D \rightarrow 3D (4)] into hydrogen-bonded networks. The type of a multicarboxylate building block has a considerable effect on the final structures of 1–4. The magnetic behavior and thermal stability of 1–4 were also investigated. Besides, these copper(II) derivatives efficiently catalyze the oxidation of cycloalkanes with hydrogen peroxide under mild conditions. The obtained products are the unique examples of copper derivatives that were assembled from H_2cpna , H_3btc , H_3cpic , and H_3cptc , thus opening up their use as multicarboxylate ligands toward the design of copper–organic architectures.



INTRODUCTION

Coordination polymers (CPs) and related metal–organic architectures are of great interest in modern inorganic and materials chemistry because of their structural features, functional properties, and variety of applications in catalysis, magnetism, sensing, luminescence, and selective sorption.^{1–10} The generation of CPs can be affected by numerous parameters such as the nature of the metal nodes, organic building blocks, and supporting ligands, stoichiometry, type of solvent, and reaction temperature.^{11–16} In particular, diverse aromatic multicarboxylic acids are commonly applied for the design of CPs because such building blocks are thermally stable and flexible and can easily satisfy the charge balance of metal nodes, thus leading to a variety of coordination modes.^{1–3,17–22} Carboxylic acids with phenylpyridine or biphenyl cores and a different arrangement of the COOH and pyridine N sites have been of particular interest,^{23–27}

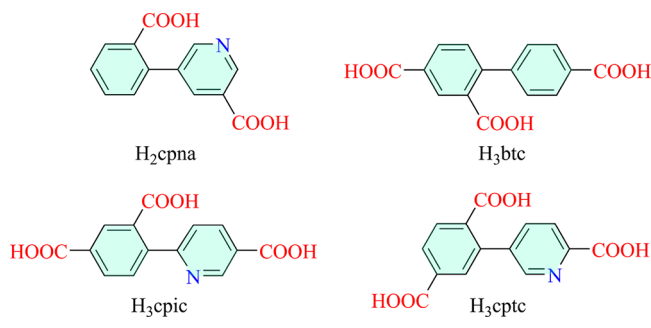
owing to a possible rotation of two aromatic cycles and variable levels of deprotonation of carboxylic acid groups. These characteristics of multifunctional carboxylic acid ligands can lead to the generation of new CPs with distinct structures.^{25–27}

In this work, an aqueous-medium system comprising copper(II) acetate, a multicarboxylic acid building block, and a crystallization mediator has been explored toward the hydrothermal generation of a new series of copper-based metal–organic architectures. The selection of copper as a metal node was governed by its low cost, rich coordination and bioinorganic chemistry, and a plethora of potential applications of copper coordination compounds, including molecular magnetism and oxidation catalysis.^{4,5,28,29}

Received: October 15, 2018

Hence, following our research line on the synthesis of novel copper-based CPs and their application in catalysis,^{4,30,31} herein we report the assembly (hydrothermal synthesis), crystal structures, thermal stability and magnetic behavior, and catalytic activity of four compounds, which are driven by different and poorly explored multicarboxylate building blocks (Scheme 1). The obtained products are 1D CPs $\{[\text{Cu}(\mu_3-$

Scheme 1. Multifunctional Carboxylic Acids



$\text{cpna})(\text{phen})\cdot\text{H}_2\text{O}\}_n$ (**1**), $\{[\text{Cu}(\mu\text{-Hbtc})(\text{phen})]\cdot\text{H}_2\text{O}\}_n$ (**2**), and $\{[\text{Cu}(\mu_3\text{-Hcpic})(\text{phen})]\cdot 2\text{H}_2\text{O}\}_n$ (**3**), as well as a discrete 0D hexacopper(II) complex, $[\text{Cu}_6(\mu\text{-Hcptc})_6(\text{phen})_6]\cdot 6\text{H}_2\text{O}$ (**4**), where $\text{H}_2\text{cpna} = 5$ -(2'-carboxyphenyl)nicotinic acid, $\text{H}_3\text{btc} =$ biphenyl-2,4,4'-tricarboxylic acid, $\text{H}_3\text{cpic} = 4$ -(5-carboxypyridin-2-yl)isophthalic acid, $\text{H}_3\text{cptc} = 2$ -(4-carboxypyridin-3-yl)terephthalic acid, and $\text{phen} = 1,10$ -phenanthroline. Their structural diversity suggests that the type of multicarboxylate block affects the structural characteristics of **1–4**. Besides, these copper(II) derivatives were explored as effective homogeneous catalysts for cycloalkane oxidation by hydrogen peroxide (H_2O_2) under mild conditions. These copper(II) catalysts are highly active without the need for an additive (strong acid), which constitutes a remarkable feature. Such a behavior can be explained by the incorporation of multicarboxylic acid building blocks into the structures of **1–4**.

Furthermore, a Cambridge Structural Database (CSD) search revealed that **1–4** are the first copper coordination compounds assembled from H_2cpna , H_3btc , H_3cpic , and H_3cptc .

EXPERIMENTAL SECTION

Reagents and Methods. All reagents were from commercial sources (analytical reagent grade) and were used as received. Elemental analyses (C/H/N) were obtained using an Elementar Vario EL elemental analyzer. Fourier transform infrared (FTIR) analyses were run using KBr disks and a Bruker EQUINOX 55 spectrometer. Thermogravimetric analyses (TGA) were carried out on a LINSEIS STA PT1600 thermal analyzer (N_2 atmosphere; 2.5 °C/min heating rate). Powder X-ray diffraction (PXRD) data were obtained on a Rigaku Dmax 2400 diffractometer ($\text{Cu K}\alpha$ radiation; $\lambda = 1.54060 \text{ \AA}$). Measurements of the magnetic susceptibility were performed on a Quantum Design MPMS XL-7 SQUID magnetometer (2–300 K; 0.1 T magnetic field strength). Prior to analysis of the data, a correction for the diamagnetic contribution was performed. The $\chi_M T$ and $1/\chi_M$ versus T plots and a description of the magnetic behavior of **1–4** are given in the Supporting Information (SI). Analysis of the reaction solutions in catalytic tests was performed by gas chromatography (GC) using an Agilent Technologies 7820A series gas chromatograph (carrier gas, He; detector, FID detector; capillary column, BP20/SGE, 30 m \times 0.22 mm \times 0.25 μm).

Synthesis and Analytical Data for **1–4.** $\{[\text{Cu}(\mu_3\text{-cpna})(\text{phen})]\cdot\text{H}_2\text{O}\}_n$ (**1**). The mixture of $\text{Cu}(\text{CH}_3\text{COO})_2\cdot\text{H}_2\text{O}$ (0.1 mmol, 20.0 mg), H_2cpna (0.1 mmol, 24.3 mg), and phen (0.1 mmol, 20.0 mg) in water (H_2O ; 10 mL) was vigorously stirred for 15 min and then transferred to a Teflon-lined stainless steel reactor (25 mL volume). It was heated for 3 days at 120 °C and then slowly cooled to ambient temperature (cooling rate: 10 °C/h). This reaction produced blue crystals, which were separated from the reaction mixture (either manually or by filtration), washed with H_2O , and dried in air to furnish product **1**. Yield: 65% (based on H_2cpna). Calcd for $\text{C}_{25}\text{H}_{17}\text{CuN}_3\text{O}_5$: C, 59.70; H, 3.41; N, 8.35. Found: C, 59.88; H, 3.39; N, 8.41. FTIR (KBr, cm^{-1}): 3492w, 3062w, 1642s, 1517w, 1492w, 1427m, 1381m, 1362s, 1284w, 1147w, 1108w, 1030w, 945w, 912w, 854 w, 769w, 723m, 671w, 645w, 534w.

$\{[\text{Cu}(\mu\text{-Hbtc})(\text{phen})]\cdot\text{H}_2\text{O}\}_n$ (**2**). CP **2** was prepared following a method described for **1** but using H_3btc instead of H_2cpna . Blue crystals were separated from the reaction mixture (either manually or

Table 1. Crystal and Structure Refinement Data for **1–4**

	1	2	3	4
chemical formula	$\text{C}_{25}\text{H}_{17}\text{CuN}_3\text{O}_5$	$\text{C}_{27}\text{H}_{18}\text{CuN}_2\text{O}_7$	$\text{C}_{26}\text{H}_{19}\text{CuN}_3\text{O}_8$	$\text{C}_{78}\text{H}_{51}\text{Cu}_3\text{N}_9\text{O}_{21}$
fw	502.95	545.98	564.98	1640.90
cryst syst	triclinic	triclinic	monoclinic	triclinic
space group	$P\bar{1}$	$P\bar{1}$	$P2_1/n$	$P\bar{1}$
$a/\text{\AA}$	9.611(3)	9.1647(9)	14.4510(11)	9.6278(6)
$b/\text{\AA}$	10.217(2)	10.4481(15)	9.9874(6)	19.0451(11)
$c/\text{\AA}$	12.399(2)	12.1649(14)	15.933(3)	19.4115(13)
α/deg	98.798(17)	94.385(11)	90	84.497(5)
β/deg	106.65(2)	93.136(9)	94.362(11)	77.500(5)
γ/deg	110.31(2)	91.169(10)	90	78.582(5)
$V/\text{\AA}^3$	1049.9(5)	1159.3(2)	2292.9(5)	3401.0(4)
T/K	293(2)	293(2)	293(2)	293(2)
Z	2	2	4	2
$D_c/\text{g cm}^{-3}$	1.591	1.561	1.637	1.602
μ/mm^{-1}	1.086	0.995	1.014	1.019
$F(000)$	514	556	1156	1674
reflms measd	6292	7552	7753	20685
unique reflms (R_{int})	3722 (0.0538)	4107 (0.1233)	4053 (0.1107)	12022 (0.0639)
GOF on F^2	0.994	0.992	0.998	0.993
$R_1 [I > 2\sigma(I)]$	0.0614	0.0896	0.0803	0.0734
$wR_2 [I > 2\sigma(I)]$	0.1185	0.1099	0.0988	0.1405

by filtration), washed with H₂O, and dried in air to furnish product 2. Yield: 60% (based on H₃btc). Calcd for C₂₇H₁₈CuN₂O₇: C, 59.40; H, 3.32; N, 5.13. Found: C, 59.57; H, 3.33; N, 5.10. FTIR (KBr, cm⁻¹): 3347w, 3063w, 1691w, 1586s, 1541w, 1517w, 1430w, 1390s, 1360w, 1256w, 1222w, 1147w, 1106w, 1002w, 909w, 874w, 857w, 793w, 776w, 723w, 690w, 660w, 551w.

$\{[\text{Cu}(\mu_3\text{-Hcpic})(\text{phen})]\cdot 2\text{H}_2\text{O}\}_n$ (3). CP 3 was prepared following a method described for 1 but using H₃cpic instead of H₂cpna. Blue crystals were separated from the reaction mixture (either manually or by filtration), washed with H₂O, and dried in air to furnish product 3. Yield: 50% (based on H₃cpic). Calcd for C₂₆H₁₉CuN₃O₈: C, 55.27; H, 3.39; N, 7.44. Found: C, 55.13; H, 3.36; N, 7.39. FTIR (KBr, cm⁻¹): 3433m, 2925w, 1694w, 1602s, 1518w, 1433w, 1362s, 1270w, 1244w, 1128w, 1050w, 1023w, 945w, 841w, 801 w, 776w, 723w, 691w, 651w, 541w.

$[\text{Cu}_6(\mu\text{-Hcptc})_6(\text{phen})_6]\cdot 6\text{H}_2\text{O}$ (4). Compound 4 was prepared following a method described for 1 but using H₃cptc instead of H₂cpna. Blue crystals were separated from the reaction mixture (either manually or by filtration), washed with H₂O, and dried in air to furnish product 4. Yield: 55% (based on H₃cptc). Calcd for C₇₈H₅₁Cu₃N₉O₂₁: C, 57.09; H, 3.13; N, 7.68. Found: C, 56.94; H, 3.15; N, 7.63. FTIR (KBr, cm⁻¹): 3318w, 3046w, 1674s, 1598s, 1517w, 1430w, 1413w, 1337s, 1286w, 1262w, 1176w, 1106w, 1048w, 950w, 858w, 776w, 724w, 695w, 648w, 567w.

X-ray Diffraction Study. For 1–4, the X-ray diffraction data were obtained using a Bruker Smart CCD diffractometer ($\lambda = 0.71073$ Å; graphite-monochromated Mo K α radiation). The SADABS program was used for an absorption correction (semiempirical). The SHELXS-97 and SHELXL-97 programs were used for solving the structures (direct methods), followed by their refinement (full-matrix least squares on F^2 procedure).³² The full-matrix least squares on F^2 procedure was applied for an anisotropic refinement of all non-hydrogen atoms. Hydrogen atoms (with the exception of those in the H₂O/OH moieties) were added in the respective calculated positions (with fixed isotropic thermal parameters) and considered in the structure factor calculations during the last stage of refinement with a full-matrix least-squares method. Hydrogen atoms of the H₂O/OH moieties were placed using difference maps with a constraint to the respective oxygen atoms. The crystal data of 1–4 are given in Table 1, while the relevant bonding and hydrogen-bonding parameters are collected in Tables S1 and S2, respectively.

Besides, to better understand the structures of 1–4, their topological analysis was carried out by applying an underlying net concept.³³ A simplified net was constructed by omitting all terminal ligands and transforming all bridging ligands into the corresponding centroids; connectivity of the bridging ligands with the copper(II) nodes via coordination bonds was maintained.

Catalytic Studies. The oxidation of alkanes under mild conditions (ambient pressure and air atmosphere) was investigated in glass reactors that were thermostated at 50 °C and equipped with the reflux condenser. The reactions were carried out under vigorous stirring in acetonitrile (MeCN) as a solvent (total volume of the reaction mixture was up to 2.5 mL). Typically, a copper(II) catalyst (5.0 μmol), trifluoroacetic acid (TFA, CF₃COOH, optional; 50 μmol as a stock solution in MeCN), an alkane substrate (1 mmol), and a GC internal standard (MeNO₂, 25 μL) were added to an MeCN solution. Then, the oxidation reaction was initiated by adding H₂O₂ (5 mmol; aqueous 50% solution). In the course of the oxidation reactions, aliquots were taken from the reaction mixtures and then treated with a minimum amount of solid triphenylphosphine (PPh₃).³⁴ Such a treatment allows reduction of the alkyl hydroperoxide (ROOH, common initial product in the oxidation of alkanes with H₂O₂) and the remaining oxidant. The obtained samples of the reaction mixture were then subjected to GC analysis. The presence of ROOH primary products was further confirmed by analyzing the selected samples twice by GC, with and without treatment with PPh₃, following a method developed by Shul'pin.³⁴ Assignment of the peaks on the gas chromatograms was performed by recording the GC plots of commercial samples; the GC internal standard was used for quantification of the products. Experiments in the absence of a

copper catalyst (blank tests) confirmed that there was no oxidation of the alkane substrates.

RESULTS AND DISCUSSION

Structural Description. *Compound 1.* CP 1 features a 1D ladder chain (Figure 1). In the asymmetric unit of 1, there is a

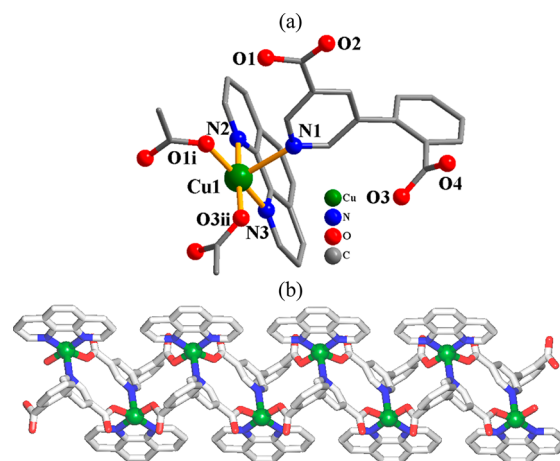
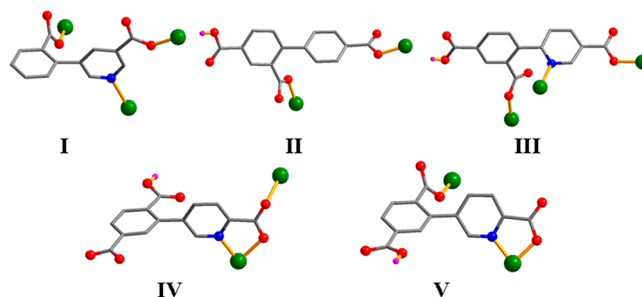


Figure 1. Fragments of the crystal structure of 1. (a) Connectivity and coordination environment of the Cu1 center (hydrogen atoms are not shown). (b) 1D ladder CP chain (view down the c axis).

Cu1 center, a μ_3 -cpna²⁻ block, a phen moiety, and a H₂O molecule of crystallization. The five-coordinate copper(II) atom is surrounded by two carboxylate oxygen donors coming from two different μ_3 -cpna²⁻ moieties, an nitrogen donor from another μ_3 -cpna²⁻ ligand, and two phen nitrogen donors, thus forming a distorted square-pyramidal {CuN₃O₂} environment with the τ parameter of 0.0792 ($\tau = 0$ or 1 for a regular square-pyramidal or trigonal-bipyramidal geometry, respectively).³⁵ The Cu–N and Cu–O bonds are in the 2.034(4)–2.382(4) and 1.934(3)–1.965(3) Å ranges, respectively (Figure 1a); these bond lengths are within the typical values for related copper(II) compounds^{22,36,37} and CPs of other metals derived from H₂cpna.²⁵ In 1, cpna²⁻ acts as a μ_3 -N,O₂ spacer, with the carboxylate groups being monodentate (mode I, Scheme 2). A

Scheme 2. Coordination Modes of μ_3 -cpna²⁻ (I), μ -Hbtc²⁻ (II), μ_3 -Hcpic²⁻ (III), and μ -Hcptc²⁻ (IV and V) in Compounds 1–4, Respectively



dihedral angle of 88.74° is observed between the rings of μ_3 -cpna²⁻. The μ_3 -cpna²⁻ blocks multiply interconnect the adjacent copper(II) centers to form a 1D ladder chain (Figure 1b). Adjacent chains then further assemble to a 2D hydrogen-bonded layer through O–H...O hydrogen bonds (Figure S1 and Table S2). From a topological viewpoint (Figure S2), the

1D ladders are assembled from 3-connected copper and μ_3 -cpna²⁻ nodes, resulting in a 3-connected underlying chain with the SP 1-periodic net (4,4)(0,2) topology. It is defined by a (4².6) point symbol.

Compound 2. Product **2** is also a 1D CP (Figure 2). An asymmetric unit of **2** has a Cu1 center, a μ -Hbtc²⁻ linker, a

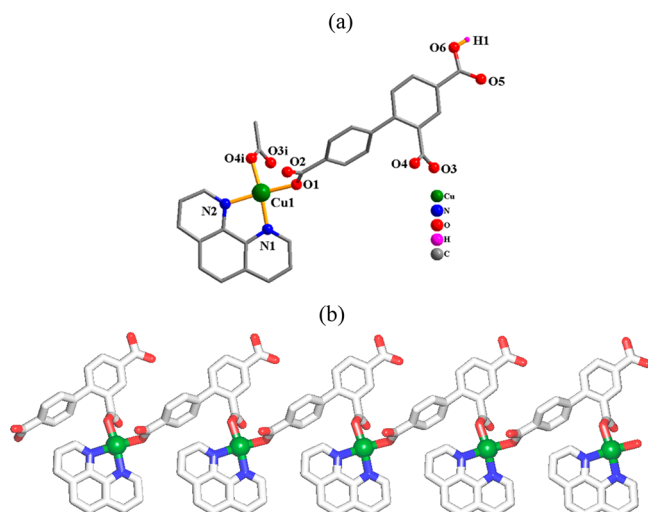


Figure 2. Fragments of the crystal structure of **2**. (a) Connectivity and coordination environment of the Cu1 center (CH hydrogen atoms are not shown). (b) 1D linear CP chain (view down the *c* axis).

phen moiety, and a crystallization H₂O molecule. The four-coordinate Cu1 atom shows a distorted {CuN₂O₂} square-planar geometry, which is taken by two oxygen donors (coming from two μ -Hbtc²⁻ blocks) and a couple of phen nitrogen donors (Figure 2a). The Cu–O [1.9429(3)–1.9435(3) Å] and Cu–N [1.986(8)–1.994(6) Å] distances are comparable to those in related copper(II) derivatives.^{26,37,38} The Hbtc²⁻ block functions as a μ -linker (mode II, Scheme 2), and its two deprotonated COO⁻ functionalities are monodentate. The dihedral angle of 53.58° is observed between the aromatic rings in μ -Hbtc²⁻. The μ -Hbtc²⁻ blocks interlink the neighboring Cu1 atoms into linear metal–organic chains having a Cu...Cu distance of 9.165 Å (Figure 2b). Such chains are classified within the 2C1 topological type (Figure S3). Besides, the 1D metal–organic chains extend into a 2D hydrogen-bonded network via the O–H...O hydrogen bonds (Table S2 and Figure S4).

Compound 3. This compound features a double 1D metal–organic chain (Figure 3). There is a Cu1 center, a μ_3 -Hcptic²⁻ block, a phen moiety, and a couple of crystallization H₂O molecules. The five-coordinate Cu1 atom forms a well-distorted square-pyramidal {CuN₃O₂} environment (τ = 0.256) that is occupied by two oxygen and one nitrogen atoms from three μ_3 -Hcptic²⁻ ligands and two phen nitrogen atoms (Figure 3a). The Cu–O [1.911(4)–1.975(4) Å] and Cu–N [1.999(6)–2.559(5) Å] distances are well comparable to those of related copper derivatives.^{36–38} In **3**, the Hcptic²⁻ spacers show a μ_3 -mode (Scheme 2, mode III), with the COO⁻ groups being monodentate; the dihedral angle that separates the aromatic functionalities attains 58.86°. The neighboring Cu1 atoms are interconnected via the oxygen and nitrogen donors from the μ_3 -Hcptic²⁻ spacers, thus forming a CP with a 1D double-chain structure (Figure 3b). These double chains are topologically similar to those in **1** (Figure

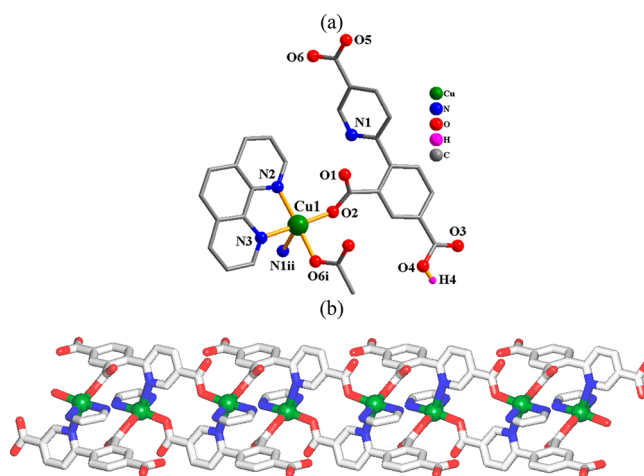


Figure 3. Fragments of the crystal structure of **3**. (a) Connectivity and coordination environment of the Cu1 center (CH hydrogen atoms are not shown). (b) 1D double chain rotated along the *c* axis (phen rings are not shown).

S5). There is also a further extension of the structure by hydrogen bonds, generating a complex 3D hydrogen-bonded net (Table S2 and Figure S6).

Compound 4. The structure of **4** has a discrete hexacopper(II) molecular unit with a cyclic tetracopper core (Figure 4). Its asymmetric unit contains three crystallographically independent copper(II) atoms, three μ -Hcptic²⁻ ligands, three phen moieties, and three crystallization H₂O molecules. All copper(II) centers are five-coordinate and possess the distorted square-pyramidal {CuN₃O₂} (Cu1), {CuN₂O₃} (Cu2), and {CuN₄O} (Cu3) geometries with τ parameters of 0.256, 0.154, and 0.128, respectively. The Cu1 center is surrounded by two carboxylate oxygen atoms and one nitrogen donor from two μ -Hcptic²⁻ ligands, in addition to two phen nitrogen donors. The Cu2 center is coordinated by three oxygen atoms and two nitrogen donors from three μ -Hcptic²⁻ blocks. A “lateral” Cu3 center is connected to the carboxylate oxygen atom from a μ -Hcptic²⁻ moiety and two pairs of phen nitrogen donors. The Cu–N and Cu–O distances are within the 1.962(5)–2.241(6) and 1.941(5)–2.298(4) Å ranges, correspondingly. All of the Hcptic²⁻ blocks act as μ -N₂O₂ spacers, and their COO⁻/COOH groups are monodentate and bidentate or remain uncoordinated (Scheme 2, modes IV and V). Dihedral angles in μ -Hcptic²⁻ vary from 89.20° to 44.50° and 44.49°. The oxygen and nitrogen donors of six μ -Hcptic²⁻ ligands interconnect the copper atoms into a discrete hexacopper(II) unit (Figure 4b), wherein the central Cu4 core is assembled from two pairs of Cu1/Cu2 nodes and μ -Hcptic²⁻ linkers (Figure S7). Besides, the intermolecular O–H...O hydrogen bonds provide an extension of the discrete Cu₆ units into a 3D hydrogen-bonded net (Table S2 and Figure S8).

Synthetic Aspects and Structural Comparison. All of the products **1–4** were synthesized using a similar hydrothermal protocol (using H₂O as a green solvent) by exploring a three-component reaction system: copper(II) acetate (metal node)–multicarboxylic acid with a phenylpyridine or biphenyl core (main building block)–1,10-phenanthroline (crystallization mediator). The effect of the type of multicarboxylate ligand containing a phenylpyridine or biphenyl core was explored, resulting in the successful crystallization of four new

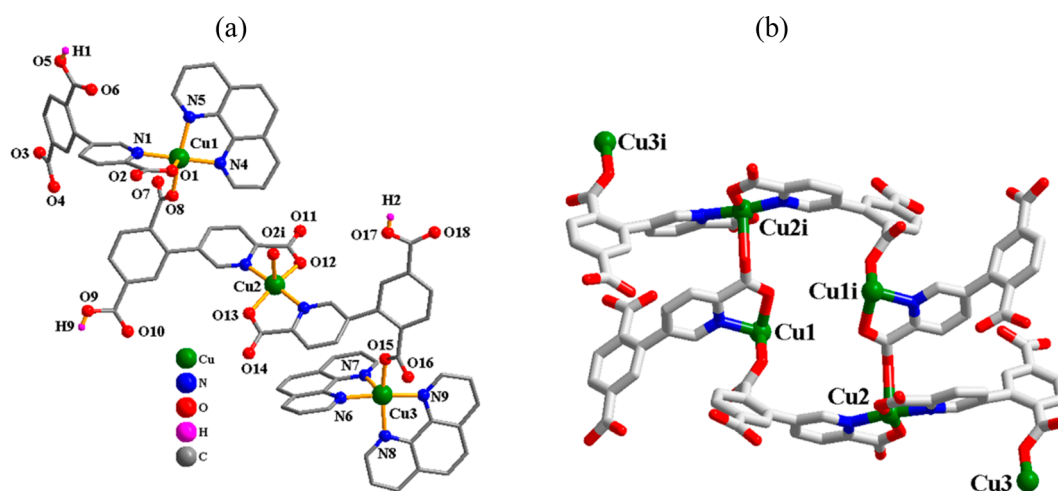


Figure 4. Fragments of the crystal structure of **4**. (a) Connectivity and coordination environment of copper centers (CH hydrogen atoms are not shown). (b) Discrete hexacopper(II) molecular unit with a cyclic Cu₄ core (phen rings are not shown).

Table 2. Selected Structural Data and Catalytic Properties for Compounds 1–4

compound	Cu coordination number {environment}	presence of uncoordinated –COOH groups	dimensionality (→ hydrogen-bonded net)	maximum yield in cycloalkane oxidation (%) ^a
{[Cu(μ ₃ -cpna)(phen)]·H ₂ O} _n (1)	5 {CuN ₃ O ₂ }	0	1D → 2D	20–30
{[Cu(μ-Hbtc)(phen)]·H ₂ O} _n (2)	4 {CuN ₂ O ₂ }	1	1D → 2D	18–22
{[Cu(μ ₃ -Hcpic)(phen)]·2H ₂ O} _n (3)	5 {CuN ₃ O ₂ }	1	1D → 3D	15–18
[Cu ₆ (μ-Hcptc) ₆ (phen) ₆]·6H ₂ O (4)	5 {CuN ₂ O ₃ }, {CuN ₃ O ₂ }, {CuN ₄ O}	1	0D → 3D	13–19

^aFor details, see Table 3.

copper(II) coordination compounds. The oxidation state of copper in all compounds is 2+, as confirmed by detailed magnetic studies (see the SI). The multicarboxylate blocks act as μ₃-spacers (in **1** and **3**) or μ-linkers (in **2** and **4**), while their COO[−] groups take a monodentate or bidentate mode. In **2–4**, one COOH group remains protonated and uncoordinated but participates in the intermolecular hydrogen-bonding interactions. The pyridyl nitrogen atoms in the cpna^{2−}, Hbtc^{2−}, and Hcptc^{2−} blocks behave as nitrogen donors for copper(II) centers in products **1**, **3**, and **4**.

To achieve the required environment of the copper(II) coordination sphere during hydrothermal synthesis, the C–C bond between the two aromatic rings in the cpna^{2−}, Hbtc^{2−}, Hcpic^{2−}, or Hcptc^{2−} blocks should have a certain degree of flexibility and rotation, as attested by the corresponding dihedral angles that are in the 44.49–89.20° range. Compounds **1–3** possess different types of 1D metal–organic chains (ladder, zigzag, or double chain, respectively), while compound **4** features a discrete 0D hexacopper(II) structure. An observed variation of the structures suggests that their hydrothermal generation depends on the type of multicarboxylate block. The copper(II) centers in **1–4** adopt square-pyramidal (in **1**, **3**, and **4**) or square-planar (in **2**) geometries. Table 2 provides a brief summary of the main structural data and catalytic properties of the obtained compounds.

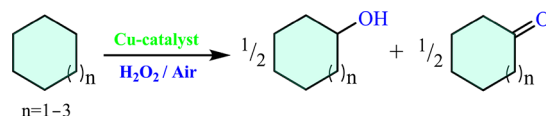
Discussion of the TGA and PXRD Data. For **1–4**, the TGA (N₂ atmosphere; 25–1000 °C) are shown in Figure S9 and briefly discussed below. CP **1** exhibits a loss of the lattice H₂O molecule (exptl, 3.4%; calcd, 3.6%) in the 104–162 °C

temperature interval; the remaining solid shows stability upon heating until 239 °C. The TGA curve of **2** indicates a thermal effect (102–163 °C), which is associated with the loss of a H₂O molecule of crystallization (exptl, 3.5%; calcd, 3.3%); heating the sample further above 227 °C provokes its decomposition. In CP **3**, mass loss due to the release of two crystallization H₂O molecules can be seen in the 105–144 °C range (exptl, 6.3%; calcd, 6.4%), followed by decomposition of the sample above 240 °C. In complex **4**, a principal thermal effect (48–108 °C) is associated with a loss of six lattice H₂O molecules (exptl, 3.4%; calcd, 3.3%). A sample obtained after dehydration maintains its stability up to 285 °C. Cu₂O is expected as a final decomposition product of **1–4** at 1000 °C. A summary of the main TGA data is provided in Table S3).

The PXRD patterns were obtained at ambient temperature using microcrystalline samples of **1–4**. Experimental PXRD plots well match the pattern calculated from the single-crystal X-ray diffraction data (Figure S10), indicating that the as-synthesized bulk materials are pure products.

Cycloalkane Oxidation Catalyzed by 1–4. The catalytic activity of all products **1–4** was studied in the mild homogeneous oxidation of C₆–C₈ cycloalkanes to give a mixture of respective alcohols and ketones (Scheme 3).

Scheme 3. Mild Catalytic Oxidation of Cycloalkanes



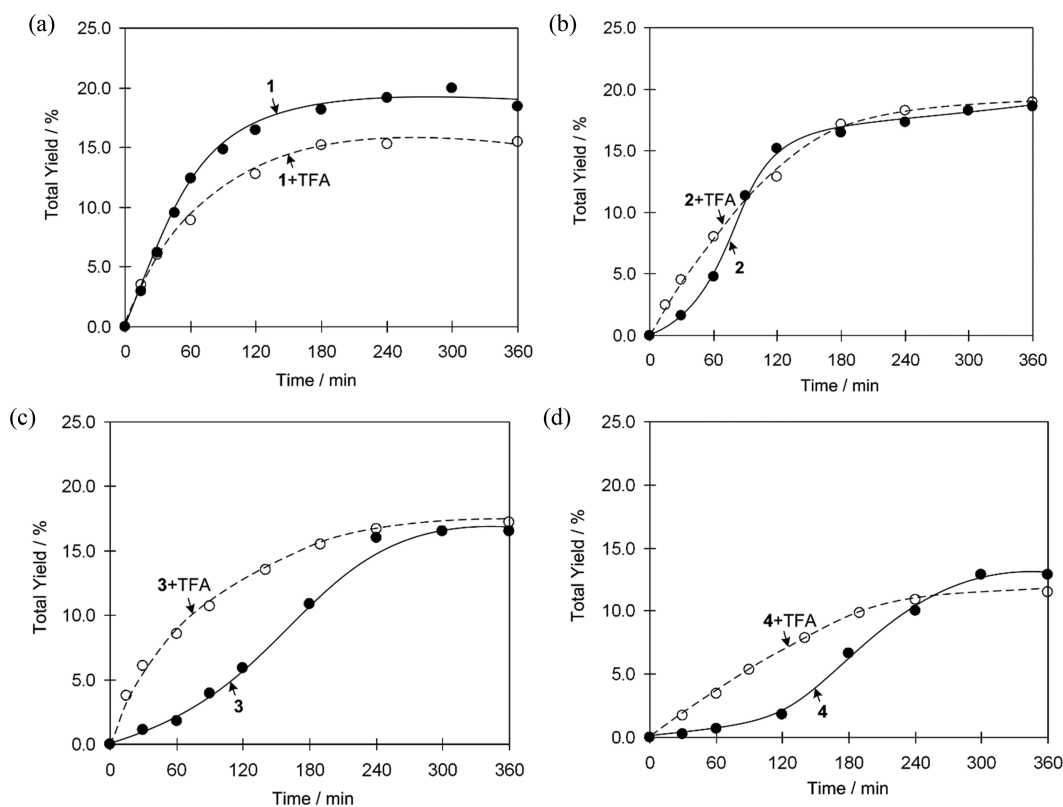


Figure 5. Cyclohexane oxidation (total yield of products, cyclohexanol, and cyclohexanone vs time) by H_2O_2 catalyzed by 1–4 (a–d) in the presence and in the absence of CF_3COOH (TFA). Conditions of the reactions: compounds 1–4, 5 μmol ; cyclohexane, 1 mmol; TFA (optional), 50 μmol ; H_2O_2 , 5 mmol; MeCN, until 2.5 mL of total reaction volume; temperature, 50 $^\circ\text{C}$.

As model substrates, cycloalkanes were chosen because of the similarity of all of their carbon atoms. Besides, such oxidation reactions are relevant in different fields^{39–41} that span from the caprolactam production (precursor of nylon-6) to the biological oxidation of alkanes with an enzyme (particulate methane monooxygenase) that contains a multicopper active center.⁴⁰ Herein, the mild oxidation of cycloalkanes was investigated in air at 50 $^\circ\text{C}$ and in MeCN/ H_2O solution, applying H_2O_2 as the oxidant (50% in H_2O). Catalytic data are shown in Figures 5 and 6 as well as in Table 3; hereinafter, the yields of products refer to the yields based on the substrate, i.e., (moles of product per mole of cycloalkane) $\times 100\%$.

Given the recognized effect of strong acids on promoting the mild oxidation of alkanes by H_2O_2 ,^{4,38,39} we studied the catalytic behavior of 1–4 in cyclohexane oxidation, with and without the use of an acid additive. As a typical acid promoter, TFA was used, and the obtained results are shown in Figure 5.

For catalyst 1, better activity (20% total product yield) is seen when the acid additive is not used (Figure 5a), whereas the total product yield is lower (15%) in the presence of TFA. The effect of TFA is negligible when using 2 as a catalyst, resulting in 18% total product yield in both systems with and without acid promoter (Figure 5b). When using the 3/TFA system, the cyclohexane oxidation is quicker, although the total yields achieved in both systems with and without TFA are similar (16–17%) after 6 h of the reaction (Figure 5c). Compound 4 shows a resembling trend but is less active than 3 (Figure 5d). In the case of catalysts 2–4, a lag period is observed (up to 120 min for 4). Such a lag period is not detected when using the TFA promoter, which facilitates the

generation of catalytically active species. The observed variations in the catalytic behavior of 1–4 are associated with their structural differences. Besides, in contrast to many other catalytic systems that require an acid promoter,^{4,30,39,41,42} all of the tested herein catalysts show similar or superior activity in the absence of acid additives. This can be explained by the presence of multicarboxylate blocks in the structure of the catalyst. Hence, further tests were performed in the absence of TFA additive.

To explore the substrate scope for these catalytic systems, we investigated the oxidation of cycloheptane and cyclooctane (Figure 6 and Table 3). Among all catalysts, the highest activity is shown by 1 for the oxidation of cycloheptane, leading to 30% total yield of the corresponding alcohol and ketone (Figure 6a). The same catalytic system is also active in the oxidation of cyclooctane with the total product yield of 22%. Interestingly, for all other catalysts (2–4), cyclooctane is the most reactive substrate (18–22% total yields), followed by cycloheptane (15–17% total yields) and cyclohexane (13–18% total yields).

In the research on the oxidative C–H functionalization of saturated hydrocarbons, the obtained yields of oxidation products (up to 30%) can be considered as very significant.^{39,41} For instance, an industrial method (DuPont) for cyclohexane oxidation uses a homogeneous catalyst (cobalt naphthenate) and proceeds with a maximum substrate conversion of ~ 5 –10%, also requiring higher temperatures and pressures.^{41d} The yields of cycloalkane oxidation products achieved herein with catalysts 1–4 are also superior or similar to the ones reported for other catalytic systems.^{4,39,42} However, because of the presence of multicarboxylic acid ligands, compounds 1–4 can

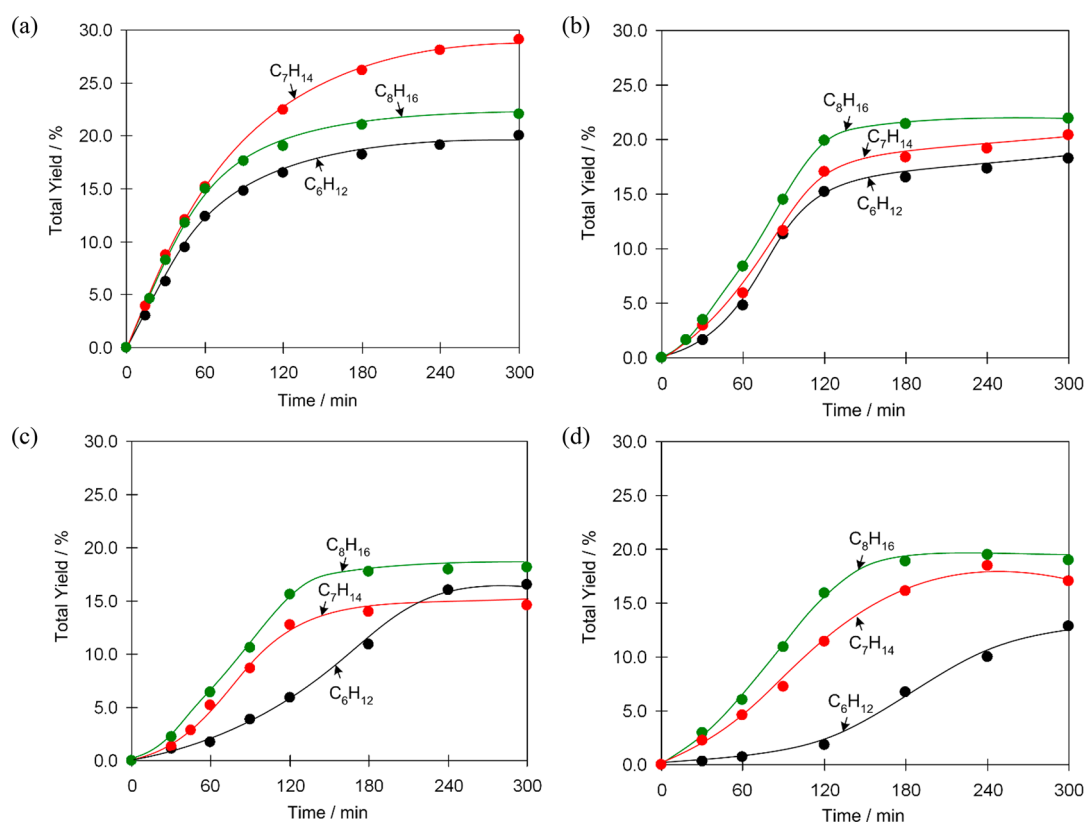


Figure 6. C₆–C₈ cycloalkane oxidation: cyclohexane, cycloheptane, and cyclooctane (alcohol and ketone total yield vs time) with H₂O₂ in the presence of catalysts 1–4 (a–d). Reaction conditions: compounds 1–4, 5 μmol; cycloalkane, 1 mmol; H₂O₂, 5 mmol; MeCN, until 2.5 mL of total reaction volume; temperature, 50 °C.

Table 3. Mild Oxidation of Cycloalkanes (C₆–C₈) in the Presence of Catalysts 1–4^a

hydrocarbon	yield (%) ^b		
	cyclic alcohol	cyclic ketone	total ^c
Catalyst 1			
cyclohexane	15.1	4.9	20.0
cycloheptane	14.7	14.8	29.5
cyclooctane	5.6	16.4	22.0
Catalyst 2			
cyclohexane	14.3	4.0	18.3
cycloheptane	8.7	11.7	20.4
cyclooctane	5.4	16.5	21.9
Catalyst 3			
cyclohexane	12.5	4.0	16.5
cycloheptane	6.6	8.0	14.6
cyclooctane	9.6	8.6	18.2
Catalyst 4			
cyclohexane	9.6	3.3	12.9
cycloheptane	6.8	10.2	17.0
cyclooctane	11.0	8.0	19.0

^aConditions of the reactions: cycloalkane, 1 mmol; catalyst 1–4, 5 μmol; H₂O₂, 5 mmol; MeCN, until 2.5 mL of total reaction volume; temperature, 50 °C; time, 5 h. ^bYields were calculated as (moles of product per mole of cycloalkane) × 100%. ^cSum of the alcohol and ketone yields.

catalyze the oxidation of cycloalkanes without the need for acid additive (promoter), which is crucial for many catalytic systems for alkane oxidation by H₂O₂ under mild conditions.^{4,30,38,42,43}

To get additional information on the selectivity parameters and the type of oxidizing species in reactions catalyzed by 1–4, the mild oxidation of a linear alkane (*n*-heptane), a substituted cycloalkane (methylcyclohexane), and stereoisomeric cycloalkanes (*cis*- and *trans*-dimethylcyclohexane) was investigated (Table 4). For all of the tested copper(II) catalysts, *n*-C₇H₁₆ oxidation occurs with no preference toward a specific secondary carbon atom at the *n*-heptane skeleton, showing a regioselectivity parameter C1:C2:C3:C4 equal to 1:4:5:5 (for 1 and 2) or 1:4:4:4 (for 3 and 4). When using methylcyclohexane as a model substrate, the bond selectivity values (1°:2°:3°) of 1:5:16 (1), 1:14:17 (2), 1:5:14 (3), and 1:5:13 (4) are quite resembling as well, thus indicating preferable oxidation of the tertiary carbon atom in comparison with the secondary carbon atoms. Besides, the application of *cis* or *trans* isomers of 1,2-dimethylcyclohexane as substrates indicates that their oxidation proceeds in a nonstereoselective way, as evidenced by the molar ratios (*trans/cis* = 0.8–0.9) among the produced tertiary alcohol isomers. Inversion of the configuration was also observed to some extent, wherein the *cis* isomers are formed in higher amounts in the oxidation of both substrates (*cis* and *trans* isomers of 1,2-dimethylcyclohexane).

Analysis of the obtained catalysis data and various selectivity parameters shows that these well compare with other copper-based systems for cycloalkane oxidation, also supporting a mechanism proceeding with HO• radicals as indiscriminate and powerful oxidizing agents.^{30,42,43} Hence, a proposed reaction mechanism (Scheme 4) involves the formation of hydroxyl radicals from H₂O₂. Then, these radicals abstract hydrogen atoms of the substrate (cycloalkane, CyH) to produce Cy• (cycloalkyl radicals). These radicals further

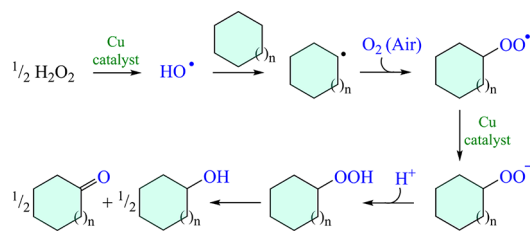
Table 4. Different Selectivity Parameters in the Oxidation of Alkanes^a

alkane and selectivity parameter	1	2	3	4
	Regioselectivity ^b			
<i>n</i> -heptane, C1:C2:C3:C4	1:4:5:5	1:4:5:5	1:4:4:4	1:4:4:4
	Bond Selectivity			
^c methylcyclohexane, 1°:2°:3°	1:5:16	1:4:17	1:5:14	1:5:13
	Stereoselectivity ^d			
<i>cis</i> -dimethylcyclohexane, trans/ <i>cis</i>	0.8	0.9	0.9	0.8
<i>trans</i> -dimethylcyclohexane, trans/ <i>cis</i>	0.8	0.8	0.8	0.9

^aReaction conditions: catalyst, 5 μmol; alkane, 1 mmol; H₂O₂, 5 mmol; MeCN, until 2.5 mL of total reaction volume; temperature, 50 °C; time, 2 h. The values of the selectivity parameters were calculated on the basis of the molar ratios of alcohol product isomers; all selectivity parameters underwent normalization, wherein a number of hydrogen atoms at every carbon center was taken into consideration.

^bParameters C1:C2:C3:C4 refer to a reactivity of hydrogen atoms at C1, C2, C3, and C4 atoms of the *n*-C₇H₁₆ skeleton. ^cParameters 1°:2°:3° refer to the reactivity of hydrogen atoms at different types (primary, secondary, or tertiary) of carbon atoms in methylcyclohexane. ^dParameters trans/*cis* refer to a molar ratio of the obtained isomeric tertiary alcohols with trans- or cis-oriented CH₃ groups.

Scheme 4. Proposed Mechanistic Pathway for the Copper-Catalyzed Oxidation of Cycloalkane Substrates, C_n (n = 1–3)



react with dioxygen (present in air or generated from H₂O₂) to form CyOO• (cycloalkylperoxy radicals). CyOO• radicals are converted into CyOOH products (cycloalkyl hydroperoxides), which represent the primary formed products; their presence in the reaction system can be evidenced from GC analyses of the reaction mixtures (Shul'pin's method).³⁴ CyOOH products decompose in the course of the reaction to give the final oxidation products (cyclic alcohols and ketones).

CONCLUSIONS

Herein we studied hydrothermal generation of copper metal–organic architectures using a three-component system: copper(II) acetate–multicarboxylic acid with a phenylpyridine or biphenyl core –1,10-phenanthroline. Four new products were generated by varying the main multicarboxylate ligand. A search of the CSD⁴⁴ confirmed that all of the obtained products constitute the first copper compounds assembled from H₂cpna, H₃btc, H₃cpic, and H₃cptc. The obtained products exhibit different metal–organic architectures, which include ladder, linear, or double 1D chains, in addition to a discrete 0D hexacopper aggregate with a cyclic Cu₄ core. The structural, topological, and hydrogen-bonding features of the obtained products were highlighted. The magnetic properties of compounds 1–4 were also studied.

Besides, compounds 1–4 efficiently catalyze the oxidation of C₆–C₈ cycloalkanes by H₂O₂ to generate the respective alcohols and ketones with total yields attaining 30%. Such yields are significant in the field of alkane C–H chemistry,^{39,41,43} particularly considering that these saturated hydrocarbons are very inert and the reactions studied herein can occur at a low temperature (50 °C) and in a MeCN/H₂O medium.

Further research on probing various types of aromatic multicarboxylic acids as versatile spacers to assemble new copper-based CPs or metal–organic frameworks with certain functional properties will be pursued in our laboratories. A special focus will be made on developing recoverable, heterogeneous catalysts based on the present type of copper(II) coordination compounds.

ASSOCIATED CONTENT

Supporting Information

The Supporting Information is available free of charge on the ACS Publications website at DOI: 10.1021/acs.inorgchem.8b02926.

Additional structural data (Tables S1 and S2), summary of the thermal analysis data (Table S3), additional structural representations (Figures S1–S8), TGA plots (Figure S9), PXRD patterns (Figure S10), and magnetic behavior (Figure S11) and its detailed discussion (PDF)

Accession Codes

CCDC 1821255–1821258 contain the supplementary crystallographic data for this paper. These data can be obtained free of charge via www.ccdc.cam.ac.uk/data_request/cif, or by emailing data_request@ccdc.cam.ac.uk, or by contacting The Cambridge Crystallographic Data Centre, 12 Union Road, Cambridge CB2 1EZ, UK; fax: +44 1223 336033.

AUTHOR INFORMATION

Corresponding Authors

*E-mail: gujzh@lzu.edu.cn. Tel.: +86-931-8915196. Fax: +86-931-8915196.

*E-mail: kirillov@tecnico.ulisboa.pt. Tel.: +351 218417178.

ORCID

Jinzhong Gu: 0000-0001-6704-7370

Zifa Shi: 0000-0001-9231-5963

Alexander M. Kirillov: 0000-0002-2052-5280

Notes

The authors declare no competing financial interest.

ACKNOWLEDGMENTS

This work was supported by the National Natural Science Foundation of China (Project 21572086), the 111 Project of MOE (111-2-17), and the Foundation for Science and Technology and Portugal 2020 (Projects IF/01395/2013/CP1163/CT005, CEECIND/03708/2017, UID/QUI/00100/2013, and LISBOA-01-0145-FEDER-029697). The paper was also prepared with support of the RUDN University Program 5-100. A.S.A. acknowledges the BL-CQE/2017-019 fellowship (UID/QUI/00100/2013). A.M.K. acknowledges the COST Action CA15106 (CHAOS).

REFERENCES

(1) For selected books, see: (a) *The Chemistry of Metal–Organic Frameworks*, 2 Vol. Set: *Synthesis, Characterization, and Applications*;

- Kaskel, S., Ed.; John Wiley & Sons, 2016. (b) *Metal–Organic Framework Materials*; MacGillivray, L. R., Lukehart, C. M., Eds.; John Wiley & Sons: Chichester, U.K., 2014. (c) Batten, S. R.; Neville, S. M.; Turner, D. R. *Coordination Polymers: Design, Analysis and Application*; Royal Society of Chemistry, 2009; p 424 pp.
- (2) (a) Lu, W.; Wei, Z.; Gu, Z.-Y.; Liu, T.-F.; Park, J.; Park, J.; Tian, J.; Zhang, M.; Zhang, Q.; Gentle, T., III; Bosch, M.; Zhou, H.-C. Tuning the structure and function of metal–organic frameworks via linker design. *Chem. Soc. Rev.* **2014**, *43*, 5561–5593. (b) Li, J.-R.; Sculley, J.; Zhou, H.-C. Metal–organic frameworks for separations. *Chem. Rev.* **2012**, *112*, 869–932. (c) Cui, Y. J.; Li, B.; He, H. J.; Zhou, W.; Chen, B. L.; Qian, G. D. Metal–organic frameworks as platforms for functional materials. *Acc. Chem. Res.* **2016**, *49*, 483–493.
- (3) (a) Yuan, S. A.; Zou, L. F.; Li, H. X.; Chen, Y. P.; Qin, J. S.; Zhang, Q.; Lu, W. G.; Hall, M. B.; Zhou, H. C. Flexible zirconium metal–organic frameworks as bioinspired switchable catalysts. *Angew. Chem., Int. Ed.* **2016**, *55*, 10776–10780. (b) DeCoste, J. B.; Peterson, G. W. Metal–organic frameworks for air purification of toxic chemicals. *Chem. Rev.* **2014**, *114*, 5695–5727.
- (4) Kirillov, A. M.; Kirillova, M. V.; Pombeiro, A. J. L. Multicopper complexes and coordination polymers for mild oxidative functionalization of alkanes. *Coord. Chem. Rev.* **2012**, *256*, 2741–2759.
- (5) (a) Loukopoulos, E.; Kallitsakis, M.; Tsoureas, N.; Abdul-Sada, A.; Chilton, N. F.; Lykakis, I. N.; Kostakis, G. E. Cu(II) Coordination Polymers as Vehicles in the A3 Coupling. *Inorg. Chem.* **2017**, *56*, 4898–4910. (b) Loukopoulos, E.; Kostakis, G. E. Recent advances of one-dimensional coordination polymers as catalysts. *J. Coord. Chem.* **2018**, *71*, 371–410. (c) Kirillova, M. V.; Kirillov, A. M.; Kuznetsov, M. L.; Silva, J. A. L.; Fraústo da Silva, J. J. R.; Pombeiro, A. J. L. Alkanes to carboxylic acids in aqueous medium: metal-free and metal-promoted highly efficient and mild conversions. *Chem. Commun.* **2009**, 2353–2355. (d) Bilyachenko, A. N.; Dronova, M. S.; Yalymov, A. I.; Lamaty, F.; Bantreil, X.; Martinez, J.; Bizet, C.; Shul'pina, L. S.; Korlyukov, A. A.; Arkhipov, D. E.; Levitsky, M. M.; Shubina, E. S.; Kirillov, A. M.; Shul'pin, G. B. Cage-like Copper(II) Silsesquioxanes: Transmetalation Reactions and Structural, Quantum Chemical, and Catalytic Studies. *Chem. - Eur. J.* **2015**, *21*, 8758–8770. (e) Armakola, E.; Colodrero, R. M. P.; Bazaga-García, M.; Salcedo, I. R.; Choquesillo-Lazarte, D.; Cabeza, A.; Kirillova, M. V.; Kirillov, A. M.; Demadis, K. D. Three-Component Copper-Phosphonate-Auxiliary Ligand Systems: Proton Conductors and Efficient Catalysts in Mild Oxidative Functionalization of Cycloalkanes. *Inorg. Chem.* **2018**, *57*, 10656–10666.
- (6) (a) Loukopoulos, E.; Abdul-Sada, A.; Viseux, E. M. E.; Lykakis, I. N.; Kostakis, G. E. Structural diversity and catalytic properties in a family of Ag(I)-benzotriazole based coordination compounds. *Cryst. Growth Des.* **2018**, *18*, 5638–5651. (b) Yu, C. X.; Hu, F. L.; Liu, M. Y.; Zhang, C. W.; Lv, Y. H.; Mao, S. K.; Liu, L. L. Construction of four copper coordination polymers derived from a tetra-pyridyl-functionalized calix[4]arene: synthesis, structural diversity and catalytic applications in the A3 (Aldehyde, Alkyne and Amine) coupling reaction. *Cryst. Growth Des.* **2017**, *17*, 5441–5448.
- (7) (a) Tăbăcaru, A.; Pettinari, C.; Galli, S. Coordination polymers and metal-organic frameworks built up with poly (tetrazolate) ligands. *Coord. Chem. Rev.* **2018**, *372*, 1–30. (b) Pettinari, C.; Tăbăcaru, A.; Galli, S. Coordination polymers and metal–organic frameworks based on poly (pyrazole)-containing ligands. *Coord. Chem. Rev.* **2016**, *307*, 1–31.
- (8) Robin, A. Y.; Fromm, K. M. Coordination polymer networks with O- and N-donors: What they are, why and how they are made. *Coord. Chem. Rev.* **2006**, *250*, 2127–2157.
- (9) (a) Restrepo, J.; Serroukh, Z.; Santiago-Morales, J.; Aguado, S.; Gómez-Sal, P.; Mosquera, M. E. G.; Rosal, R. An Antibacterial Zn–MOF with Hydrazinebenzoate Linkers. *Eur. J. Inorg. Chem.* **2017**, *2017*, 574–580. (b) Zheng, X. F.; Zhou, L.; Huang, Y. M.; Wang, C. G.; Duan, J. G.; Wen, L. L.; Tian, Z. F.; Li, D. F. A series of metal-organic frameworks based on 5-(4-pyridyl)-isophthalic acid: selective sorption and fluorescence sensing. *J. Mater. Chem. A* **2014**, *2*, 12413–12422. (c) Lu, K. D.; Aung, T.; Guo, N. N.; Weichselbaum, R.; Lin, W. B. Nanoscale metal–organic frameworks for therapeutic, imaging, and sensing applications. *Adv. Mater.* **2018**, *30*, 1707634.
- (10) (a) Castro, K. A. D. F.; Figueira, F.; Mendes, R. F.; Cavaleiro, J. A. S.; Neves, M. G. P. M. S.; Simões, M. M. Q.; Almeida Paz, F. A.; Tomé, J. P. C.; Nakagaki, S. Copper–Porphyrin–Metal–Organic Frameworks as Oxidative Heterogeneous Catalysts. *ChemCatChem* **2017**, *9*, 2939–2945. (b) Wu, W.; Kirillov, A. M.; Yan, X.; Zhou, P.; Liu, W.; Tang, Y. Enhanced separation of potassium ions by spontaneous K⁺-induced self-assembly of a novel metal–organic framework and excess specific cation– π interactions. *Angew. Chem., Int. Ed.* **2014**, *53*, 10649–10653.
- (11) Gu, J. Z.; Wu, J.; Lv, D. Y.; Tang, Y.; Zhu, K. Y.; Wu, J. C. Lanthanide coordination polymers based on 5-(2'-carboxyphenyl) nicotinate: syntheses, structure diversity, dehydration/hydration, luminescence and magnetic properties. *Dalton Trans.* **2013**, *42*, 4822–4830.
- (12) (a) Manna, P.; Das, S. K. Perceptive approach in assessing rigidity versus flexibility in the construction of diverse metal–organic coordination networks: synthesis, structure, and magnetism. *Cryst. Growth Des.* **2015**, *15*, 1407–1421. (b) Jaremko, Ł.; Kirillov, A. M.; Smoleński, P.; Pombeiro, A. J. L. Engineering coordination and supramolecular copper-organic networks by aqueous medium self-assembly with 1,3,5-triaza-7-phosphaadamantane (PTA). *Cryst. Growth Des.* **2009**, *9*, 3006–3010.
- (13) Zhang, J. Y.; Shi, J. X.; Chen, L. Y.; Jia, Q. X.; Deng, W.; Gao, E. Q. N-donor auxiliary ligand-directed assembly of Co^{II} compounds with a 2,2'-dinitro-biphenyl-4,4'-dicarboxylate ligand: structures and magnetic properties. *CrystEngComm* **2017**, *19*, 1738–1750.
- (14) Xu, W.; Si, Z. X.; Xie, M.; Zhou, L. X.; Zheng, Y. Q. Experimental and theoretical approaches to three uranyl coordination polymers constructed by phthalic acid and N,N-Donor bridging ligands: crystal structures, luminescence, and photocatalytic degradation of tetracycline hydrochloride. *Cryst. Growth Des.* **2017**, *17*, 2147–2157.
- (15) Zang, S. Q.; Dong, M. M.; Fan, Y. J.; Hou, H. W.; Mak, T. C. W. Four cobaltic coordination polymers based on 5-Iodo-isophthalic Acid: halogen-related interaction and solvent effect. *Cryst. Growth Des.* **2012**, *12*, 1239–1246.
- (16) Wan, J.; Cai, S. L.; Zhang, K.; Li, C. J.; Feng, Y.; Fan, J.; Zheng, S. R.; Zhang, W. G. Anion- and temperature-dependent assembly, crystal structures and luminescence properties of six new Cd(II) coordination polymers based on 2,3,5,6-tetrakis(2-pyridyl)pyrazine. *CrystEngComm* **2016**, *18*, 5164–5176.
- (17) Xue, Y. S.; Jin, F. Y.; Zhou, L.; Liu, M. P.; Xu, Y.; Du, H. B.; Fang, M.; You, X. Z. Structural diversity and properties of coordination polymers built from a rigid octadentate carboxylic acid. *Cryst. Growth Des.* **2012**, *12*, 6158–6164.
- (18) Sahu, J.; Ahmad, M.; Bharadwaj, P. K. Structural diversity and luminescence properties of coordination polymers built with a rigid linear dicarboxylate and Zn(II)/Pb(II) Ion. *Cryst. Growth Des.* **2013**, *13*, 2618–2627.
- (19) Wang, S. L.; Hu, F. L.; Zhou, J. Y.; Zhou, Y.; Huang, Q.; Lang, J. P. Rigidity versus flexibility of ligands in the assembly of entangled coordination polymers based on bi- and tetra carboxylates and N-Donor ligands. *Cryst. Growth Des.* **2015**, *15*, 4087–4097.
- (20) Zhang, J. Y.; Shi, J. X.; Cui, P. H.; Yao, Z. J.; Deng, W. Structural diversity and catalytic properties of five Co₂(COO)₄ cluster-based coordination polymers modified with R-isophthalic acid (R = H, NO₂CH₂OH and tBu). *CrystEngComm* **2017**, *19*, 5038–5047.
- (21) Lin, Z. J.; Han, L. W.; Wu, D. S.; Huang, Y. B.; Cao, R. Structure versatility of coordination polymers constructed from a semirigid tetracarboxylate ligand: syntheses, structures, and photoluminescent properties. *Cryst. Growth Des.* **2013**, *13*, 255–263.
- (22) Gu, J. Z.; Liang, X. X.; Cai, Y.; Wu, J.; Shi, Z. F.; Kirillov, A. M. Hydrothermal assembly, structures, topologies, luminescence, and magnetism of a novel series of coordination polymers driven by a trifunctional nicotinic acid building block. *Dalton Trans.* **2017**, *46*, 10908–10925.

- (23) Song, J. F.; Jia, Y. Y.; Zhou, R. S.; Li, S. Z.; Qiu, X. M.; Liu, J. Six new coordination compounds based on rigid 5-(3-carboxyphenyl)-pyridine-2-carboxylic acid: synthesis, structural variations and properties. *RSC Adv.* **2017**, *7*, 7217–7226.
- (24) Maza, W. A.; Padilla, R.; Morris, A. J. Concentration dependent dimensionality of resonance energy transfer in a post-synthetically doped morphologically homologous analogue of UiO-67 MOF with a ruthenium(II) polypyridyl complex. *J. Am. Chem. Soc.* **2015**, *137*, 8161–8168.
- (25) (a) Gu, J. Z.; Gao, Z. Q.; Tang, Y. pH and auxiliary ligand influence on the structural variations of 5-(2'-carboxylphenyl) nicotinate coordination polymers. *Cryst. Growth Des.* **2012**, *12*, 3312–3323. (b) Lv, D.-Y.; Gao, Z.-Q.; Gu, J.-Z.; Ren, R.; Dou, W. Synthesis, crystal structures, magnetic and luminescent properties of nickel(II) and cadmium(II) coordination polymers bearing 5-(2'-carboxylphenyl) nicotinate ligands. *Transition Met. Chem.* **2011**, *36*, 313–318.
- (26) Gu, J. Z.; Liang, X. X.; Cui, Y. H.; Wu, J.; Kirillov, A. M. Exploring 4-(3-carboxyphenyl)picolinic acid as a semirigid building block for the hydrothermal self-assembly of diverse metal–organic and supramolecular networks. *CrystEngComm* **2017**, *19*, 117–128.
- (27) Gu, J. Z.; Cui, Y. H.; Liang, X. X.; Wu, J.; Lv, D. Y.; Kirillov, A. M. Structurally distinct metal-organic and H-bonded networks derived from 5-(6-carboxypyridin-3-yl)isophthalic acid: coordination and template effect of 4,4'-bipyridine. *Cryst. Growth Des.* **2016**, *16*, 4658–4670.
- (28) (a) *Bioinorganic Chemistry of Copper*; Karlin, K. D., Tyeklar, Z., Eds.; Springer: Berlin, 2012. (b) *Copper–Oxygen Chemistry*; Itoh, S., Rokita, S., Eds.; Wiley: New York, 2011.
- (29) (a) Pandolfo, L.; Pettinari, C. Trinuclear copper(II) pyrazolate compounds: a long story of serendipitous discoveries and rational design. *CrystEngComm* **2017**, *19*, 1701–1720. (b) Carlotto, S.; Pandolfo, L.; Casarin, M. Trinuclear Cu(II) complexes from the classic $[\text{Cu}_2(\text{RCOO})_4(\text{H}_2\text{O})_2]$ lantern complex and pyrazole: a DFT modelling of the reaction path. *Inorg. Chim. Acta* **2018**, *470*, 93–99.
- (30) Fernandes, T. A.; Santos, C. I. M.; André, V.; Klak, J.; Kirillova, M. V.; Kirillov, A. M. Copper(II) coordination polymers self-assembled from aminoalcohols and pyromellitic acid: highly active pre-catalysts for the mild water-promoted oxidation of alkanes. *Inorg. Chem.* **2016**, *55*, 125–135.
- (31) (a) Dias, S. S. P.; André, V.; Klak, J.; Duarte, M. T.; Kirillov, A. M. Topological Diversity of Supramolecular Networks Constructed from Copper(II) Aminoalcohol Blocks and 2,6-Naphthalenedicarboxylate Linkers: Self-Assembly Synthesis, Structural Features, and Magnetic Properties. *Cryst. Growth Des.* **2014**, *14*, 3398–3407. (b) Gu, J.-Z.; Wen, M.; Liang, X.; Shi, Z.-F.; Kirillova, M. V.; Kirillov, A. M. Multifunctional Aromatic Carboxylic Acids as Versatile Building Blocks for Hydrothermal Design of Coordination Polymers. *Crystals* **2018**, *8*, 83.
- (32) (a) Sheldrick, G. M. A program for automatic solution of crystal structure. *Acta Crystallogr., Sect. A: Found. Crystallogr.* **1990**, *A46*, 467–473. (b) Sheldrick, G. M. *SHELXS-97, A Program for X-ray Crystal Structure Solution and SHELXL-97, A Program for X-ray Crystal Structure Refinement*; Göttingen University: Göttingen, Germany, 1997.
- (33) (a) Blatov, V. A. Multipurpose crystallochemical analysis with the program package TOPOS. *IUCrCompComm Newsletter* **2006**, *7*, 4–38. (b) Blatov, V. A.; Shevchenko, A. P.; Proserpio, D. M. Applied topological analysis of crystal structures with the program package topospro. *Cryst. Growth Des.* **2014**, *14*, 3576–3586.
- (34) (a) Shul'pin, G. B. New trends in oxidative functionalization of carbon–hydrogen bonds: a review. *Catalysts* **2016**, *6*, 50. (b) Shul'pin, G. B. Metal-catalyzed hydrocarbon oxygenations in solutions: the dramatic role of additives: a review. *J. Mol. Catal. A: Chem.* **2002**, *189*, 39–66. (c) Shul'pin, G. B. Metal-catalysed hydrocarbon oxidations. *C. R. Chim.* **2003**, *6*, 163–178. (d) Shul'pin, G. B. Hydrocarbon oxygenations with peroxides catalyzed by metal compounds. *Mini-Rev. Org. Chem.* **2009**, *6*, 95–104.
- (35) Addison, A. W.; Rao, T. N.; Reedijk, J.; Van Rijn, J.; Verschoor, G. C. Synthesis, structure, and spectroscopic properties of copper(II) compounds containing nitrogen-sulphur donor ligands: the crystal and molecular structure of aqua[1,7-bis(N-methylbenzimidazol-2'-yl)-2,6-dithiaheptane] copper(II) perchlorate. *J. Chem. Soc., Dalton Trans.* **1984**, *7*, 1349–1356.
- (36) Feng, Y. F.; Tang, Q.; Luo, K. L.; Wu, J. Q.; Zhang, Z.; Liang, Y. N.; Liang, F. P. Controllable assembly of Cu(II) coordination compounds based on a flexible zwitterionic benzimidazole–dicarboxylate ligand: synthesis, structural diversity, reversible SCSC transformation and magnetic properties. *CrystEngComm* **2017**, *19*, 5442–5459.
- (37) Chattopadhyay, K.; Shaw, B. K.; Saha, S. K.; Ray, D. Unique trapping of paddlewheel copper(II) carboxylate by ligand-bound $\{\text{Cu}_2\}$ fragments for $[\text{Cu}_6]$ assembly. *Dalton Trans.* **2016**, *45*, 6928–6938.
- (38) Dias, S. S. P.; Kirillova, M. V.; André, V.; Klak, J.; Kirillov, A. M. New tricopper(II) cores self-assembled from aminoalcohol biobuffers and homophthalic acid: synthesis, structural and topological features, magnetic properties and mild catalytic oxidation of cyclic and linear C_5 – C_8 alkanes. *Inorg. Chem. Front.* **2015**, *2*, 525–537.
- (39) (a) Kirillov, A. M.; Shul'pin, G. B. Pyrazinecarboxylic acid and analogs: highly efficient co-catalysts in the metal-complex-catalyzed oxidation of organic compounds. *Coord. Chem. Rev.* **2013**, *257*, 732–754. (b) Olah, G. A.; Molnar, A. *Hydrocarbon Chemistry*; Wiley, 2003.
- (40) Sirajuddin, S.; Rosenzweig, A. C. Enzymatic oxidation of methane. *Biochemistry* **2015**, *54*, 2283–2294.
- (41) (a) Bäckvall, J. E., Ed. *Modern oxidation methods*; Wiley: New York, 2011. (b) Shilov, A. E.; Shul'pin, G. B. *Activation and catalytic reactions of saturated hydrocarbons in the presence of metal complexes*; Kluwer Academic Publishers: Dordrecht, The Netherlands, 2000. (c) Olah, G. A.; Molnar, A. *Hydrocarbon chemistry*; Wiley: New York, 2003. (d) Schuchardt, U.; Cardoso, D.; Sercheli, R.; Pereira, R.; da Cruz, R. S.; Guerreiro, M. C.; Mandelli, D.; Spinace, E. V.; Pires, E. L. Cyclohexane oxidation continues to be a challenge. *Appl. Catal., A* **2001**, *211*, 1–17.
- (42) (a) Gupta, S.; Kirillova, M. V.; Guedes da Silva, M. F. C.; Pombeiro, A. J. L.; Kirillov, A. M. Alkali metal directed assembly of heterometallic V^n/M ($\text{M} = \text{Na}, \text{K}, \text{Cs}$) coordination polymers: Structures, topological analysis, and oxidation catalytic properties. *Inorg. Chem.* **2013**, *52*, 8601–8611. (b) Dias, S. S. P.; Kirillova, M. V.; André, V.; Klak, J.; Kirillov, A. M. New tetracopper(II) cubane cores driven by a diamino alcohol: Self-assembly synthesis, structural and topological features, and magnetic and catalytic oxidation properties. *Inorg. Chem.* **2015**, *54*, 5204–5212.
- (43) (a) Shul'pin, G. B. C–H functionalization: thoroughly tuning ligands at a metal ion, a chemist can greatly enhance catalyst's activity and selectivity. *Dalton Trans.* **2013**, *42*, 12794–12818. (b) Shul'pin, G. B. Selectivity enhancement in functionalization of C–H bonds: A review. *Org. Biomol. Chem.* **2010**, *8*, 4217–4228.
- (44) Groom, C. R.; Bruno, I. J.; Lightfoot, M. P.; Ward, S. C. The Cambridge Structural Database. *Acta Crystallogr., Sect. B: Struct. Sci., Cryst. Eng. Mater.* **2016**, *B72*, 171–179.